The Journal of Clinical Endocrinology & Metabolism, 2021, Vol. 106, No. 10, 2949–2961
doi:10.1210/clinem/dgab410
Clinical Research Article

Clinical Research Article

Central Insulin Modulates Dopamine Signaling in the Human Striatum

Stephanie Kullmann,[1,2,3,†] Dominik Blum,[4,†] Benjamin Assad Jaghutriz,[1,2,3] Christoph Gassenmaier,[5] Benjamin Bender,[6] Hans-Ulrich Häring,[1,2,3] Gerald Reischl,[7] Hubert Preissl,[1,2,3,8,9] Christian la Fougère,[4,10] Andreas Fritsche,[1,2,3] Matthias Reimold,[4,10] and Martin Heni[1,2,3,11]

[1]Institute for Diabetes Research and Metabolic Diseases of the Helmholtz Center Munich at the University of Tübingen, Germany; [2]German Center for Diabetes Research (DZD), Tübingen, Germany; [3]Department of Internal Medicine, Division of Endocrinology, Diabetology and Nephrology, Eberhard Karls University Tübingen, Tübingen, Germany; [4]Department of Nuclear Medicine and Clinical Molecular Imaging, Eberhard-Karls-University Tübingen, Tübingen, Germany; [5]Department of Internal Medicine, Division of Hematology, Oncology, Clinical Immunology and Rheumatology, Eberhard Karls University Tübingen, Tübingen, Germany; [6]Department of Diagnostic and Interventional Neuroradiology, University Hospital Tübingen, Tübingen, Germany; [7]Werner Siemens Imaging Center, Department of Preclinical Imaging and Radiopharmacy, Eberhard Karls University Tübingen, Tübingen, Germany; [8]Institute for Diabetes and Obesity, Helmholtz Diabetes Center at Helmholtz Zentrum München, German Research Center for Environmental Health (GmbH), Neuherberg, Germany; [9]Department of Pharmacy and Biochemistry, Institute of Pharmaceutical Sciences, Eberhard Karls University Tübingen, Tübingen, Germany; [10]Cluster of Excellence iFIT (EXC 2180) "Image Guided and Functionally Instructed Tumor Therapies", University of Tübingen, Germany; and [11]Institute for Clinical Chemistry and Pathobiochemistry, Department for Diagnostic Laboratory Medicine, University Hospital Tübingen, Tübingen, Germany

ORCiD numbers: 0000-0001-9951-923X (S. Kullmann); 0000-0002-8859-4661 (H. Preissl); 0000-0002-8462-3832 (M. Heni).

[†]Contributed equally.

Abbreviations: BOLD, blood oxygenation level-dependent; BP_{nd}, [^{11}C]-raclopride binding potential; CBF, cerebral blood flow; fALFF, fractional amplitude of low-frequency fluctuation; FC, functional connectivity; fMRI, functional magnetic resonance imaging; MNI, Montreal Neurological Institute; MRI, magnetic resonance imaging; NAc, nucleus accumbens; PET, positron emission tomography; PFC, prefrontal cortex; pFWE, p-value family-wise error corrected; ROI, region of interest; TI, inversion time; VTA, ventral tegmental area; WHO, World Health Organization.

Received: 4 January 2021; Editorial Decision: 3 June 2021; First Published Online: 15 June 2021; Corrected and Typeset: 5 July 2021.

Abstract

Objective: Activity in the dopaminergic pathways of the brain is highly sensitive to body weight and metabolic states. Animal studies show that dopamine neurons are important targets for the metabolic hormone insulin with abolished effects in the insulin-resistant

ISSN Print 0021-972X ISSN Online 1945-7197
Printed in USA

state, leading to increases in body weight and food intake. In humans, the influence of central acting insulin on dopamine and effects of their interplay are still elusive.

Research Design and Methods: We investigated whether central administered insulin influences dopaminergic activity in striatal regions and whole-brain neural activity. Using a positron emission tomography (PET)/magnetic resonance imaging (MRI) hybrid scanner, we simultaneously performed [^{11}C]-raclopride-PET and resting-state functional MRI in 10 healthy normal-weight men after application of intranasal insulin or placebo on 2 separate days in a randomized, placebo-controlled, blinded, crossover trial.

Results: In response to central insulin compared with placebo administration, we observed greater [^{11}C]-raclopride binding potential in the bilateral ventral and dorsal striatum. This suggests an insulin-induced reduction in synaptic dopamine levels. Resting-state striatal activity was lower 15 and 30 minutes after nasal insulin compared with placebo. Functional connectivity of the mesocorticolimbic circuitry associated with differences in dopamine levels: individuals with a stronger insulin-induced effect on dopamine levels showed a stronger increase in functional connectivity 45 minutes after intranasal insulin.

Conclusions: This study indicates that central insulin modulates dopaminergic tone in the striatum, which may affect regional brain activity and connectivity. Our results deepen the understanding of the insulin-dopamine interaction and the complex network that underlies the regulation of whole-body metabolism.

Key Words: insulin, dopamine, PET, fMRI, striatum, obesity

Obesity and type 2 diabetes are serious public health concerns because of their increasing prevalence and comorbidities. The brain is increasingly recognized to play a prominent role in the development of these noncommunicable diseases. Insulin action in the brain brings about multiple behavioral and metabolic effects with consequences for body weight regulation, as well as motivation and cognition (1-4). Markedly reduced insulin action (ie, insulin resistance) is a hallmark feature of obesity and type 2 diabetes.

Insulin receptors are expressed throughout the brain with downstream functions best characterized in the hypothalamus (5-8). The importance of insulin functions beyond homeostatic control in the hypothalamus and its impact on reward, eating behavior, and whole-body metabolism has recently received growing interest. Thereby, the dopaminergic circuitry is recognized as a crucial target of insulin (9, 10).

Dopamine is the central neurotransmitter of the mesocorticolimbic system, in which signals from the ventral tegmental area (VTA) are transmitted to the ventral and dorsal striatum and the prefrontal cortex (PFC) to regulate especially reward-related functions. Animal studies have found insulin to interact with dopamine in both the VTA and the striatum (10, 11). Administration of insulin directly into the VTA in rodents suppresses ingestive behavior (10). Specifically in a positive energy balance state, food seeking (12) and the consumption of high-fat food (13) are decreased. Thus, insulin in the VTA may decrease the rewarding aspects of food intake (10).

The intranasal administration of insulin provides the possibility to investigate central insulin action in the absence of major peripheral side effects (14, 15). Experimental studies in rats showed that intranasally administered insulin is transported rapidly along extraneuronal routes through the olfactory and trigeminal pathway and acts within multiple sites of the brain (16-19). Likewise, in humans, insulin is detectable in the cerebrospinal fluid within 1 hour of intranasal administration (20).

In line with findings from basic science, current studies in humans illuminate the role of central acting insulin in the brain showing tremendous impact on whole-body metabolism and long-term weight regulation (2, 21). Using intranasal delivery to the human brain, insulin modulates regional brain activity as well as connections of the hypothalamus and predominantly brain regions of the mesocorticolimbic circuitry (15, 22-26), with the most prominent response to 160 U of regular human insulin (15, 26, 27). Nonetheless, it is still unknown whether central insulin action actually involves the modulation of dopaminergic tone in humans. To address this question, we performed simultaneous positron emission tomography (PET)/magnetic resonance imaging (MRI) in 10 healthy men using [^{11}C]-raclopride, a dopamine D2/3 receptor ligand widely used for assessment of synaptic levels of dopamine

based on competition and subsequent (noncompetitive) effects (28-30) and resting state functional MRI (fMRI). To stimulate insulin action, we used the intranasal delivery of insulin to the brain in a randomized, placebo-controlled, blinded, crossover trial.

Research Design and Methods

Study design

We performed combined PET/MRI measurements in 10 healthy normal weight men (age, 27 ± 3 years; body mass index, 23.6 ± 2.3 kg/m²; Homeostatic Model Assessment of Insulin Resistance, 1.8 ± 1.1) after application of intranasal insulin or placebo on 2 separate days after an overnight fast (with a mean time lag of 35 ± 11 days) (see Fig. 1 for study design; for consort graph see Kullmann et al (31)). In the fasting state, concentrations of circulating insulin as well as incretin hormones are low. During PET data acquisition, resting-state blood oxygenation level-dependent (BOLD) fMRI and pulsed arterial spin labeling were assessed at 3 different time points after nasal spray application (15, 30, and 45 minutes after spray). Blood samples were taken before nasal spray application and 30 and 60 minutes after nasal spray application. Eating behavior (trait questionnaires) was assessed using the German Three Factor Eating Questionnaire to determine cognitive restraint, disinhibition, and hunger (32), and the trait version of the Food Craving Questionnaire (33). Mood was assessed on each measurement day using the World Health Organization-5 (WHO-5) well-being index (34) (data shown elsewhere (31)).

The local ethics committee approved the protocol, and informed written consent was obtained from all participants. All participants were students at the University of Tübingen and were recruited using broadcast emails. The study was preregistered at clinicaltrials.gov (NCT03637075). Participants underwent thorough medical examination including blood analyses at screening; they were healthy, did not smoke, take any medication, or suffer from psychiatric, neurological, or metabolic diseases. Participants were instructed to refrain from vigorous exercise 3 days before each measurement.

Power calculation

To evaluate the effect of intranasal insulin versus placebo on [^{11}C]-raclopride binding potential (BP_{nd}) and resting-state brain activity, we used an effect size of 1 to calculate a total sample size of n = 10 for matched pairs (α error probability of 0.05, power of 0.8). This effect size was achieved in recent fMRI studies investigating the effect of intranasal insulin compared with placebo on resting-state brain activity (1, 24).

Application of intranasal insulin/placebo

The insulin and placebo spray were prepared in nasal sprays and administered in a randomized, blinded fashion on 2 separate study days. Participants received on 1 day 160 U of insulin (Insulin Actrapid; Novo Nordisk, Bagsvaerd, Denmark) and on the other day vehicle as placebo (35). Plasma glucose was measured by glucose oxidase method. Serum insulin, C-peptide, cortisol, testosterone, prolactin, and GH were measured using commercial immunoassay with ADVIA Centaur XP Immunoassay System (Siemens Healthineers, Eschborn, Germany).

Image acquisition

[^{11}C]-raclopride, which specifically binds to dopamine D2 and D3 receptors (36), was prepared under a manufacturing authorization in good manufacturing practices quality.

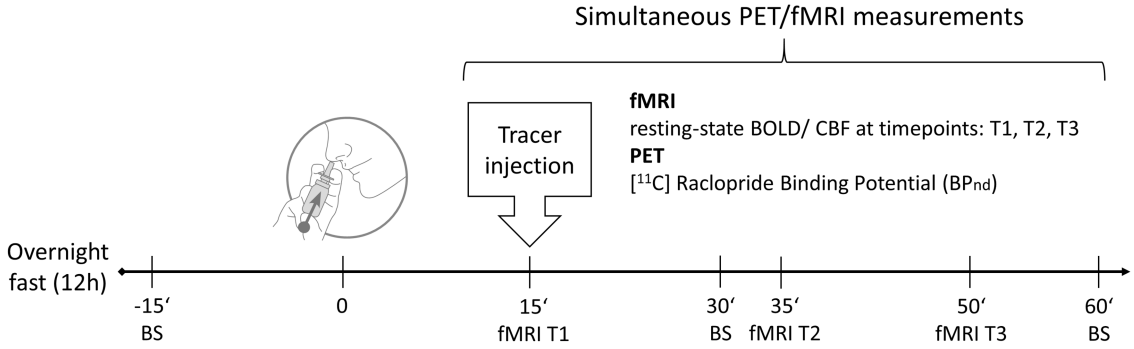

Figure 1. Scheme of test procedure. Fifteen minutes after nasal spray application, [^{11}C]-raclopride PET data acquisition was performed for 1 hour. Resting-state fMRI was acquired at 3 time points after spray application. Blood samples (BS) were taken before (-15 minutes), 30 minutes, and 60 minutes after nasal spray application. The order of placebo and insulin spray application was counterbalanced over participants. fMRI, functional magnetic resonance imaging; PET, positron emission tomography.

Synthesis was performed as described before (37), yielding a radiochemical purity >95% and a molar activity > 50 GBq/µmol in accordance with the respective European Pharmacopoeia Monograph (Raclopride ([11C]methoxy) injection, No. 1924). After intranasal administration of insulin or placebo, the subject was placed within the hybrid PET/MRI scanner (3 Tesla Biograph mMR; Siemens Healthineers Erlangen/Germany, 12-channel head coil) with 3 fiducial markers attached to the scull to support realignment. Fifteen minutes after insulin/placebo application, 376 ± 79 MBq of [^{11}C]-raclopride were injected intravenously as bolus (10 seconds) followed by a 60-minute emission scan. Dynamic PET images (12 frames × 10 seconds, 12 frames × 20 seconds, 12 frames × 60 seconds, 14 frames × 180 seconds) were reconstructed using ordinary Poisson OSEM (3 iterations, 21 subsets) with ultrashort echo time-based attenuation correction and a 4-mm Gauss filter and stored in a 256 × 256 × 127 voxel grid with voxel size 1.4 × 1.4 × 2.0 mm³.

Whole-brain functional MRI data were collected by using gradient echo-planar imaging sequences at three time points after spray application. The following sequence was used: repetition time = 2 seconds, echo time = 30 ms, field of view = 192 mm², matrix 64 × 64, flip angle 90°, voxel size 3 × 3 × 4.25 mm^3, and slice thickness 3.4 mm with 25% gap between slices; images were acquired in ascending order. Each brain volume comprised 30 axial slices and each functional run contained 160 image volumes, resulting in a total acquisition time of 5.20 minutes for each resting state measurement. To acquire cerebral blood flow (CBF), pulsed arterial spin labeling images were obtained with a proximal inversion with control for off-resonance effects–quantitative imaging of perfusion by using a single subtraction sequence as recently described (1). A total of 16 axial slices with a slice thickness of 3 mm (3.6-mm gap) were acquired in ascending order, resulting in an acquisition time of 3.54 minutes. Each measurement consisted of 79 alternating tag and control images with the following imaging parameters: inversion time (TI), TI1 = 700 ms, TI2 = 1800 ms, repetition time = 3000 ms, echo time = 13 ms, in-plane resolution = 3 × 3 mm^2, field of view = 192 mm, matrix size 64 × 64, and flip angle = 90°.

In addition, high-resolution T1-weighted anatomical images (MPRAGE GRAPPA2: 1 × 1 × 1 mm^3, flip angle = 9°, TI = 900, repetition time = 2300 ms, echo time = 2.98 ms) of the brain were obtained.

Image processing of PET data

All PET image processing was done with MATLAB R2017 and Statistical Parametric Mapping (SPM12, http://www.fil.ion.ucl.ac.uk/spm). For each PET scan, we first calculated a reference image by summing all frames from 5 to 8 minutes after injection. All following frames were then realigned to the reference image. Next, the reference image was coregistered to T1-MRI of the first visit, which was used for spatial normalization to the Montreal Neurological Institute (MNI) space using the standard SPM algorithm. Realignment, coregistration, and normalization parameters were then used to resample all PET frames to match the voxel grid (121 × 145 × 121) and voxel size (1.5 mm cubic voxels) of the brain label atlas from Neuromorphometrics, Inc.

PET kinetic modelling and region-of-interest analysis

PET target measure was the "in vivo" binding potential BP_{nd} (38), which is proportional to the concentration of available binding sites and is a standard PET measure to assess displacement effects. BP_{nd} was calculated in predefined striatal regions of interest (ROI) as well as for each voxel, using the multilinear reference tissue model 2. The cerebellum was used as a reference region, using a single washout rate k'_2 from cerebellum and a time t^* = 10 minutes after which the system response was considered monoexponential (39). Apart from the binding potential, the time course of radiotracer concentration in the brain depends on perfusion and the extraction fraction of [^{11}C]-raclopride. Central insulin may affect these parameters. In pharmacokinetic modelling, these 2 parameters are combined to a single rate constant (K1) and modelling is used to estimate BP_{nd} independent from K1.

The following ROIs were extracted from the brain label atlas: ventral striatum (ie, nucleus accumbens), caudate nucleus, putamen (Fig. 2), and cerebellum. Caudate nucleus and putamen were combined as dorsal striatum.

Image processing of fMRI resting-state data

Resting-state fMRI data were analyzed with the Data Processing Assistant for Resting-State fMRI (40) (http://www.restfmri.net), which is based on SPM12 and Resting-State fMRI Data Analysis Toolkit (41) (REST, http://www.restfmri.net). Functional images were realigned, coregistered to the T1 structural image, normalized to voxel size: 3 × 3 × 3 mm^3 and smoothed with a 3-dimensional isotropic Gaussian kernel (full width at half maximum, 6 mm). Normalization was performed using the MNI template with DARTEL. To the functional images, a temporal filter (0.01-0.08 Hz) was applied to reduce low-frequency drifts and high-frequency physiological noise. Nuisance regression was performed using white matter, cerebrospinal fluid, and the 6 head motion parameters as covariates. No participant had head motion with more than 2.0 mm maximum

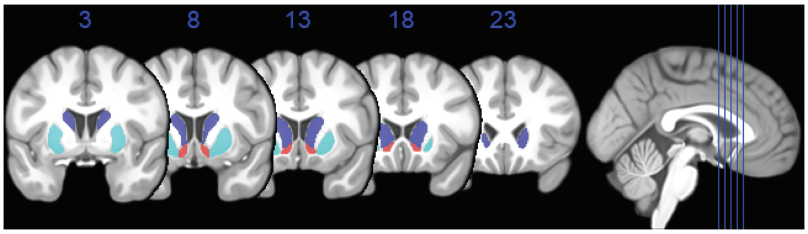

Figure 2. Regions of interest for PET analysis (displayed on an anatomical template): binding potential (BP_{nd}) was extracted from the caudate (blue), putamen (cyan), and the ventral striatum/nucleus accumbens (red). Caudate and putamen together are referred to as dorsal striatum. PET, positron emission tomography.

displacement or 2.0° of any angular motion. To investigate resting-state brain activity, we calculated the fractional amplitude of low-frequency (0.01-0.08 Hz) fluctuations (fALFF) of the BOLD signal (42). fALFF is a resting-state fMRI parameter that measures the magnitude of the regional brain activity, which is based on amplitude and intensity (42). Specifically, the regional intensity of spontaneous BOLD fluctuations is quantified by the power spectrum in the low frequency range (0.009-0.08 Hz) and regularized by the power in the whole frequency range (0-0.25 Hz) (42).

Image processing of CBF data

Image preprocessing was performed by using the ASLtbx (43) with SPM12 (Wellcome Trust Centre for Neuroimaging). Functional images were motion corrected, coregistered to the individual anatomical image, and smoothed (full width at half maximum, 6 mm). Perfusion images were generated by calculating the control-tag differences by using surround subtraction. For accurate CBF quantification (mL × $100g^{-1}$ × min^{-1}), we used a unique M0 value extracted from an ROI in the cerebrospinal fluid. For absolute perfusion quantification, the general kinetic model was applied. The high-resolution T1-weighted image was normalized and the resulting parameter file was used with the individual coregistered CBF maps in normalized space (3 × 3 × 3 mm). The field of view of the ASL sequence varied between measurement time points; hence, only parts of the striatum were measured. A mask was used to obtain all voxels assessed during all measurement time points. CBF of the striatum (mainly caudate nucleus) and global CBF were extracted to calculate normalized CBF values.

Statistics

Hormone measurements

To compare the 2 experimental conditions, treatment × time interactions were tested by repeated measures ANOVA using JMP 14 (SAS Institute, Cary, NC, USA).

PET analysis

The primary analysis of PET was to assess BP_{nd} to nasal insulin compared with placebo in 2 striatal regions of interest (ventral striatum, dorsal striatum). To this end, paired *t* tests were carried out to investigate the effect of insulin compared with placebo on BP_{nd}, as a measure of synaptic dopamine. We considered effects significant if they survived correction for 2 independent tests according to the method of Bonferroni-Holm ($P < 0.05$, 1-sided *t* test). For descriptive reasons, we also calculated *t* tests for the 2 subregions of the dorsal striatum (ie, caudate and putamen). For further correlation analyses, we calculated $\Delta BP_{nd} = BP_{nd\ insulin} - BP_{nd\ placebo}$ as a measure of insulin-induced modulation of synaptic dopamine.

Resting-state fMRI analysis

Resting-state BOLD was acquired after insulin and placebo spray to assess resting-state activity and functional connectivity between major nodes of the dopaminergic mesocorticolimbic circuitry at 3 time points after insulin and placebo spray application. For the fALFF maps, repeated measurement ANOVA/full factorial model was performed in SPM12 (within-subject factor spray: insulin and placebo, within-subject factor time: T1, T2, and T3). Significant clusters were extracted for post hoc analyses. A statistical threshold of $p < 0.05$ voxel-level family-wise error (FWE) corrected was applied on a whole-brain level and small volume corrected for the striatal regions (combined ROI for ventral and dorsal striatum).

Based on recent findings on intranasal insulin action on resting-state functional connectivity (2), we included 5 ROIs of the mesocorticolimbic circuitry: the bilateral ventral tegmental area, the dorsal striatum (caudate and putamen), the ventral striatum (ie, the nucleus accumbens), the lateral hypothalamus, and the medial PFC. The average BOLD time course was obtained from these bilateral regions and the correlation coefficient map was calculated between the 5 ROIs. The resulting correlation coefficient map was converted by a Fisher's r-to-z transformation to

improve normality. Functional connectivity (FC) values (z-transformed correlation coefficients) of the 10 possible connections were extracted to calculate $\Delta FC = FC_{insulin} - FC_{placebo}$ as a measure of insulin-induced functional connectivity differences in the dopaminergic mesocorticolimbic circuitry at each time point. To quantify resting-state activity, fALFF values were extracted of the striatum to calculate $\Delta fALFF = fALFF_{insulin} - fALFF_{placebo}$.

Further statistical analyses were carried out in SPSS (version 25, IBM, Armonk, NY, USA). We investigated whether there is a link between insulin-induced differences in dopamine levels (based on ΔBP_{nd}) and functional connectivity as well as resting-state activity. For this purpose, Pearson correlations were calculated between ΔBP_{nd} in the ventral striatum and ΔFC and ΔfALFF at each time point. A P value of < 0.01 was considered significant (P value corrected for number of ROIs).

Results

PET ROI analysis

The primary analysis was to assess the effect of intranasal insulin compared with placebo on BP_{nd} in 2 striatal regions of interest (ventral striatum, dorsal striatum) (Fig. 2). In all striatal ROI, BP_{nd} was higher after intranasal insulin compared with placebo administration with the most significant difference in the ventral striatum ($T(9) = 2.3$, $P = 0.022$, see Table 1). Fig. 3 illustrates the differences in BP_{nd} in the ventral and dorsal striatum between insulin and placebo day. In an exploratory analysis, we correlated behavioral trait measurements with differences in BP_{nd} in the ventral and dorsal striatum. Cognitive restraint correlated with differences in BP_{nd} of the dorsal and ventral striatum ($r = 0.646$, $P = 0.04$; $r = 0.690$, $P = 0.03$, respectively) (31). Subjective psychological well-being on insulin day correlated with differences in BP_{nd} of the dorsal and ventral striatum ($r = 0.647$, $P = 0.04$; $r = 0.841$, $P = 0.002$, respectively); and differences in well-being between measurement days (ΔWHO-5) correlated with differences in BP_{nd} of the dorsal and ventral striatum ($r = 0.524$, $P = 0.120$; $r = 0.814$, $P = 0.004$, respectively) (31). Hence, those with higher cognitive restraint and subjective well-being responded with a greater difference in BP_{nd} to intranasal insulin compared with placebo (31). BP_{nd} were adjusted for subjective well-being based on the WHO-5 questionnaire of each measurement day using linear regression. Adjusted BP_{nd} values were reanalyzed using a paired t test. In both ventral and dorsal striatum, adjusted BP_{nd} was higher after intranasal insulin compared with placebo administration ($P < 0.005$) (for details see supplementary material (31)).

Resting-state CBF response

No main effect of spray, time, or spray by time was observed on striatal blood flow ($P > 0.05$) (31).

Resting-state fMRI response using fALFF

We observed a significant main effect of spray (insulin < placebo) in the caudate (MNI coordinates X: 6, Y: 12, Z: 9, $p_{FWE} < 0.05$, small volume corrected). Post hoc analyses showed a significant difference in fALFF values (reflecting the magnitude of resting-state fMRI signal) for insulin compared with placebo at time point 15 and 30 minutes

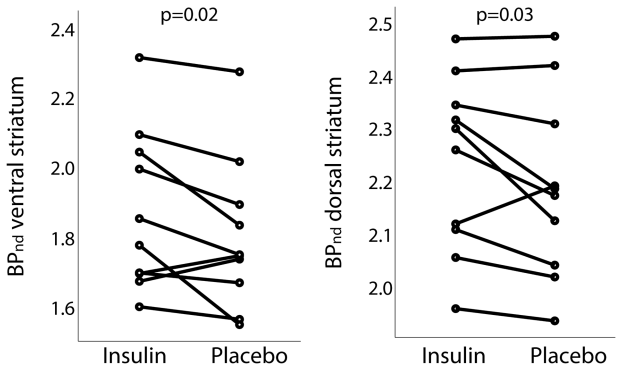

Figure 3. [^{11}C]-raclopride binding potential (BP_{nd}) in ventral and dorsal striatum on insulin and placebo day. Line diagrams show significant higher BP_{nd} in ventral and dorsal striatum after insulin compared with placebo spray application.

Table 1. Effect of intranasal insulin and placebo on BP_{nd}

	BP_{nd} (mean ± SD)			
	After insulin spray	After placebo spray	t value (df = 9)	P value*
Ventral striatum/NAc	1.88 ± 0.22	1.81 ± 0.22	2.34	0.02
Dorsal striatum	2.23 ± 0.16	2.19 ± 0.17	2.06	0.03
Caudate	1.82 ± 0.15	1.78 ± 0.15	1.88	0.05
Putamen	2.55 ± 0.22	2.49 ± 0.23	2.08	0.03

[^{11}C]-Raclopride binding potential (BP_{nd}) in all analyzed regions of interest. Dorsal striatum composed of putamen and caudate (*paired t test, 1-sided).
NAc, nucleus accumbens.

after spray application ($P < 0.05$) (Fig. 4). No main effect of time or interaction between spray and time was observed in striatal regions ($p_{FWE} > 0.05$).

Correlation analyses between resting-state fMRI and BP_{nd}

To associate dopamine levels with resting-state activity of the striatum, ΔBP_{nd} of the ventral striatum was correlated with ΔfALFF at each time point. We identified a significant correlation between ΔBP_{nd} of the ventral striatum and ΔfALFF 15 minutes after spray application ($r = -0.673$, $P = 0.03$). Hence, individuals with higher BP_{nd} in ventral striatum showed lower resting-state activity in the ventral striatum 15 minutes after intranasal insulin compared with placebo spray application (Fig. 5).

Differences in functional connectivity ($\Delta FC = FC_{insulin} - FC_{placebo}$ at each of the 3 time points) between the bilateral VTA, dorsal striatum, ventral striatum, hypothalamus, and medial PFC were calculated and correlated with ΔBP_{nd} of the ventral striatum. We identified a significant correlation between ΔBP_{nd} of the ventral striatum and ΔFC 45 minutes after spray application (Fig. 6) for the following connections: ventral striatum-VTA functional connectivity ($r = 0.717$, $P = 0.01$), ventral striatum-hypothalamus functional connectivity ($r = 0.666$, $P = 0.01$), and PFC-VTA functional connectivity ($r = 0.806$, $P = 0.002$). Hence, individuals with higher BP_{nd} in ventral striatum (indicating insulin-induced reductions of dopaminergic activity) showed stronger functional connectivity within the dopaminergic network. This was detected approximately 1 hour after insulin administration.

Metabolic parameters

Although serum insulin and C-peptide decreased over time, neither the course of serum insulin nor C-peptide was significantly different between study days ($p_{MANOVA\ treatment \times time} = 0.4$ and 0.06, respectively). Concurrently, the course of plasma glucose was comparable between nasal insulin and placebo conditions ($p_{MANOVA\ treatment \times time} = 0.4$) (Fig. 7).

Serum prolactin, testosterone, and GH did not change during the experiment and no effect of nasal insulin vs placebo was detected ($p_{MANOVA\ treatment \times time} = 0.7$, 0.2, and 1.0, respectively) (Fig. 7). Although serum cortisol concentrations decreased over time, this was not different between the 2 conditions ($p_{MANOVA\ treatment \times time} = 0.1$).

Discussion

In this study, we investigated central insulin action on dopaminergic tone in the human brain. We report higher dopamine D2 receptor availability in the ventral and dorsal striatum after application of intranasal insulin as compared with placebo, indicating an insulin-induced reduction of dopaminergic neurotransmission. Furthermore, the simultaneous PET and fMRI measurements enabled us to detect differences in resting-state activity and functional

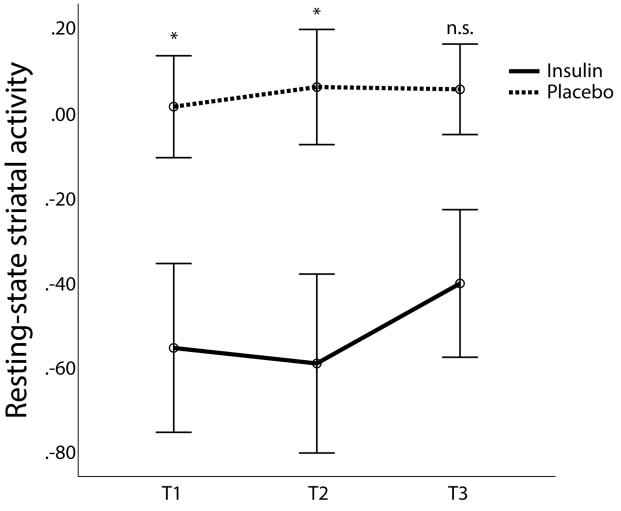

Figure 4. Central insulin effect on resting-state activity (based on fALFF) in the striatum (ie, caudate) on insulin and placebo day 15, 30, and 45 minutes after spray application. fALFF reflects the magnitude of the resting-state activity. *$P < 0.05$ for paired t test insulin vs. placebo. fALFF, fractional amplitude of low-frequency fluctuations.

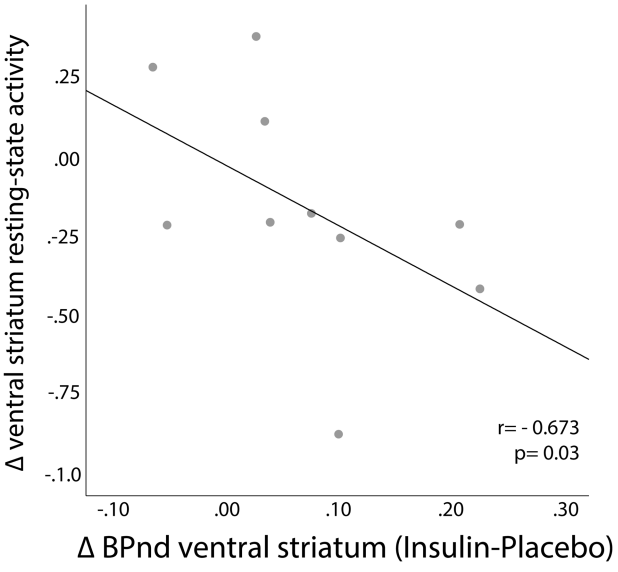

Figure 5. Central insulin effect on dopamine signaling in the ventral striatum is associated with resting-state activity in the striatum. In particular, insulin-induced differences in BP_{nd} (insulin – placebo) are negatively correlated with differences in resting-state activity (insulin – placebo) 15 minutes after intranasal application. BP_{nd}, [^{11}C]-raclopride binding potential.

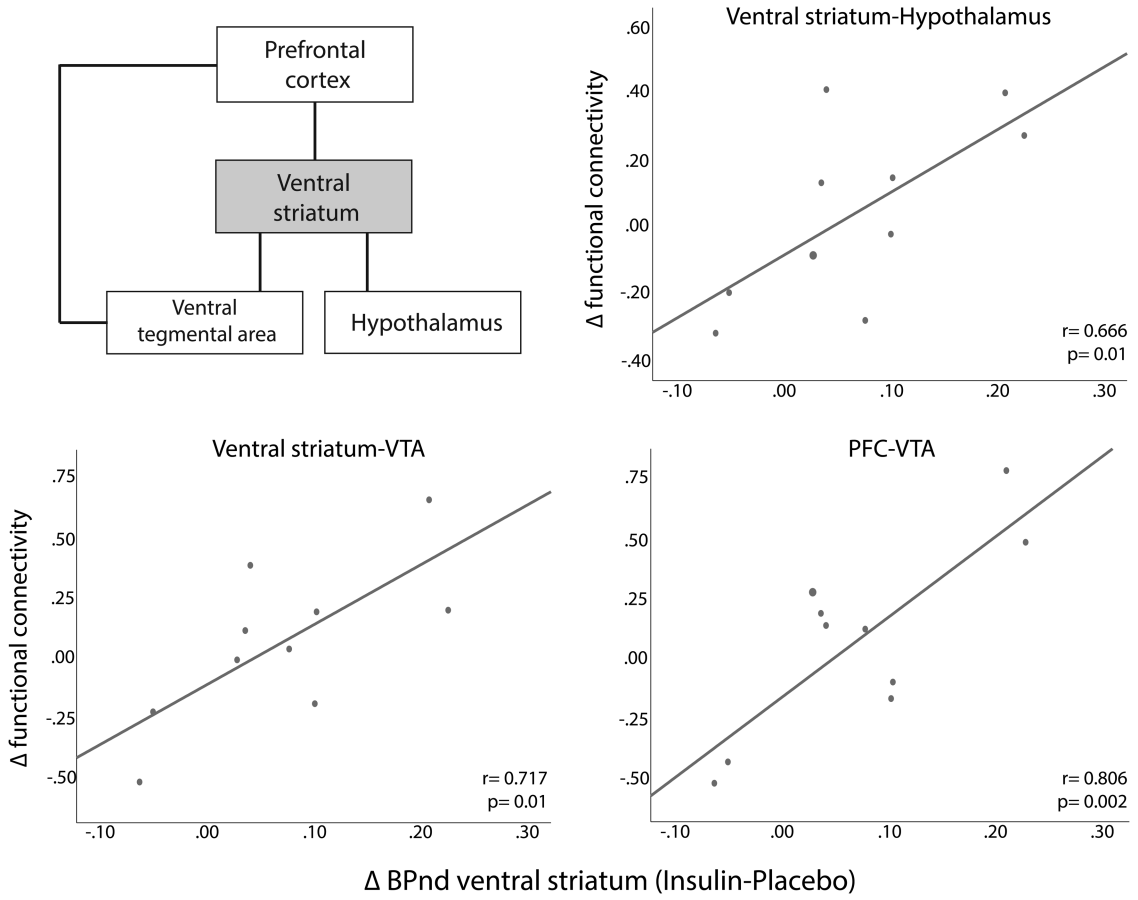

Figure 6. Central insulin effect on dopamine signaling in the ventral striatum is associated with altered functional connectivity in the dopaminergic mesocorticolimbic circuitry. Schematic overview on top left shows functional connections influenced by insulin-dopamine interaction. In particular, insulin-induced differences in BP_{nd} are associated with differences in functional connectivity (insulin – placebo day) between ventral striatum, hypothalamus, VTA and PFC measured 45 minutes after intranasal application. BP_{nd}, [^{11}C]-raclopride binding potential; PFC, prefrontal cortex; VTA, ventral tegmental area.

connectivity within and beyond the mesocorticolimbic network that were associated with insulin's modulation of striatal dopaminergic tone. This highlights how the insulin-dopamine interaction is embedded in a complex brain network that regulates eating-related reward and whole-body metabolism. Furthermore, our current results underline the notion that insulin acts specifically on the central dopaminergic system. Prolactin and GH concentrations did not change in response to intranasal insulin. Hence, the tuberoinfundibular pathway, which regulates pituitary hormone release (44), was not affected by central-acting insulin. This is in line with previous intranasal insulin studies (15) as well as with results from the conditional knockout of central insulin receptors in mice (45). Based on the limited spatial resolution, it is not possible to differentiate between central dopaminergic pathways as the mesocorticolimbic and nigrostriatal pathway. Hence, we refer to the mesocorticolimbic circuitry to interpret our findings, which may include different projections of the dopaminergic pathway.

Previous studies show that insulin acts in the human hypothalamus to induce satiety and improve peripheral glucose metabolism (2, 46). The hypothalamus in turn influences major dopaminergic projections within the mesocorticolimbic circuitry, thereby linking energy homeostasis with reward (9, 10). These dopaminergic neurons include projections from the substantia nigra/VTA to the ventral and dorsal striatum, as well as projections from the VTA to the amygdala, hippocampus, and medial prefrontal cortex (2). In this regard, both the ventral striatum and the VTA are major target areas of hypothalamic inputs.

In line with this conceptualization, previous human fMRI studies demonstrate that central insulin influences hypothalamic, striatal, and prefrontal activity (15, 22-24, 47). In response to 160 U of intranasal insulin, striatal activity decreases approximately 30 minutes after application under resting conditions (15, 22, 48) as well as in response to food cues, possibly dampening the reinforcing value of food (25). Participants report less food craving and hunger and rate high caloric foods as less

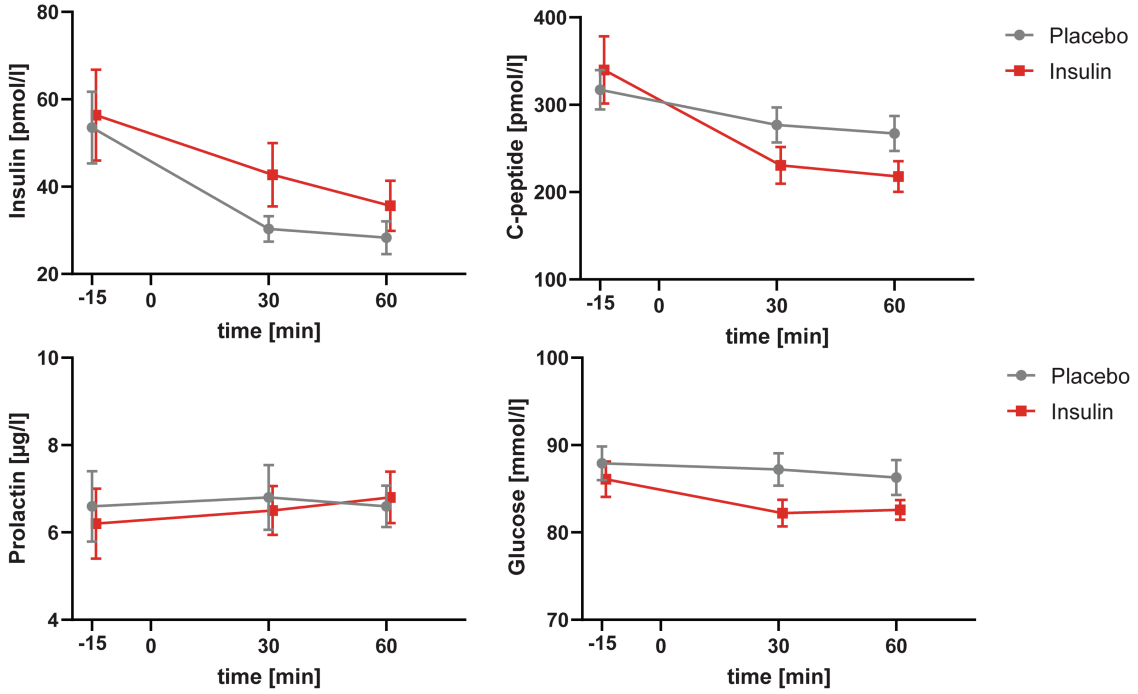

Figure 7. Metabolic parameters during experiment. Nasal insulin or placebo was administered at time point 0. The graphs show changes in insulin, C-peptide, prolactin, and glucose. No effect of nasal insulin vs placebo was detected ($p_{MANOVA\ treatment \times time} > 0.05$).

palatable after intranasal insulin administration (1, 25, 49). Hence, persons with a stronger insulin response in the mesocorticolimbic circuitry show more pronounced effects on food reward. Likewise, in the current study, we identified lower resting state activity in the striatum 15 and 30 minutes after spray application and higher functional connectivity 45 minutes after spray application, which significantly correlated with the magnitude of differences in dopamine signaling. These temporal dynamics of central insulin have also been reported in rodent studies (reviewed elsewhere [10, 11]). Administration of insulin directly into the nucleus accumbens (NAc) (analogue to the ventral striatum in humans) leads to rapid increases in local dopamine concentrations, which are completely reversed by insulin washout (11). Insulin action in the VTA, on the other hand, is long-lasting and suppresses dopamine release in the NAc (50). Similarly, insulin application directly into the rodent cerebrospinal fluid initially increases dopamine release in the NAc followed by a delay of around 30 minutes, which leads to a decrease of dopamine concentrations (10, 51). Thus, central insulin action plays a prominent role in the reinforcement and motivation for food. Of course, these temporal dynamic changes in central insulin action need to be interpreted with caution as they may reflect differences in physiological and pharmacological manipulations (11). Nonetheless, a complex and time-sensitive interaction between insulin and dopamine appears to be required to ensure proper regulation of the mesocorticolimbic system. In a postprandial state, when insulin levels are physiologically rising, intra-VTA insulin decreases food-seeking behavior and the rewarding properties of food (10, 12, 13). Concurrently, we found lower dopamine levels in response to central insulin, reflected by higher ^{11}C-raclopride binding. Both D2 receptor density and endogenous dopamine concentrations influence the binding potential. Because of the short intervention time and within-subject design, we did not expect significant changes in D2 receptor density. Hence, we postulate that central insulin decreases tonic concentrations of dopamine or the ability to induce phasic burst (10). Nonetheless, we cannot rule out that differences in [^{11}C]-raclopride binding could be due to insulin action on the postsynaptic neuron by mechanisms other than altered neurotransmitter levels.

Moreover, previous PET studies in humans using [^{11}C]-raclopride have shown an immediate increased dopamine release in the ventral striatum in response to food intake (52), glucose ingestion (53), food taste (54-56), and viewing high-caloric food images (57). This further substantiates that striatal dopamine is a key player in reinforcement and motivation for food. We hypothesize that low central insulin concentrations facilitate this role of striatal dopamine in the fasting state, increasing food seeking and motivation. During the postprandial rise of insulin, as mimicked in the current study, central insulin may lead to more long-lasting effect, promoting neuroplasticity of the mesocorticolimbic circuitry as seen by insulin-induced long-term depression

in the VTA-dopamine neurons in rodents (11). In human neuroimaging studies, functional connectivity is used a as a marker of neuroplasticity. Previous studies have shown central insulin-induced enhanced functional connectivity from and to the prefrontal cortex (26, 49), which significantly mediated subjective feeling of hunger (49). Concomitantly, we now detected strengthened functional connections between the hypothalamus and the mesocorticolimbic circuitry in response to insulin, which appear to be modulated by dopaminergic tone. Hence, besides eating behavior and metabolism, central insulin action may influence also mood and cognitive functions (58, 59). Interestingly, we found measures of mood and cognitive control over food intake to correlate with central insulin induced differences in BP_{nd}. Persons with better cognitive restraint and higher subjective well-being showed the strongest insulin-induced modulation of dopamine levels. Although BP_{nd} has been demonstrated to be linked to subjective well-being (28, 60, 61) and eating behavior (54), little is known of the effect of insulin-dopamine interaction on mood and cognition. Epidemiological evidence revealed higher risk for dementia and mood disorders in diabetes. Recently, insulin resistance in the brain has been proposed as a joined feature between metabolic and cognitive dysfunction (58). Whether disturbances in central insulin-dopamine interaction are pathophysiological involved is currently not known in humans. Animal models of obesity, however, have shown that insulin receptors on dopaminergic neurons are desensitized, leading to an abolished effect of insulin in the VTA and NAc (see review (10)) and a further increase in body weight and food intake (62).

Disturbances in insulin signaling in the human brain also affects peripheral metabolism and body fat distribution (21, 22, 63-71). Diminished central insulin action in the striatum was detected in those genetically prone to obesity when less dopamine receptors are available (23). Moreover, accumulating evidence suggests that central insulin action in the dopamine circuitry is linked to peripheral metabolism (10, 22, 59, 64, 65). PET recordings show reduced peripheral insulin sensitivity and impaired beta-cell function in persons with low dopamine levels (66, 72). Furthermore, central insulin action in the striatum improves postprandial peripheral metabolism in insulin-sensitive persons (73), possibly by modulating dopamine levels (10, 59, 64, 74). This gives merit to further investigate the effect of central disturbances in insulin action on peripheral glucose metabolism in obesity-associated insulin resistance.

The limited sample size of our current work did not allow us to investigate specific subgroups. Previous studies on central insulin action show sex-specific effects on eating behavior and metabolism (14). Hence, it is possible that our findings are specific to men. Moreover, further behavioral assessments are necessary to evaluate the central insulin-dopamine interaction on food intake and eating behavior. Because we did not include those with obesity or diabetes, we cannot directly test the impact of brain insulin resistance in the interplay of insulin and dopamine in the human brain, but draw conclusions in this regard mainly on the basis of previous findings. Because we did not perform a metabolic challenge test, but studied our participants in the fasted state, we cannot directly address the impact of our current findings on whole-body metabolism, as most brain-derived modulation of peripheral metabolism requires a postprandial milieu with elevated circulating insulin (73).

Taken together, we provide experimental evidence that central insulin modulates dopaminergic activity in the ventral and dorsal striatum. This response was closely linked to striatal resting-state activity and functional connectivity in the mesocorticolimbic circuitry that regulates reward as well as eating behavior and is likely involved in the postprandial control of whole-body glucose metabolism. Our current results deepen the understanding of the complex circuitry that underlies the regulation human behavior and metabolism by insulin. Further studies need to evaluate central insulin action on the dopamine circuitry in those with obesity, and diabetes and its contribution to the proper control of reward, eating, and metabolism.

Acknowledgments

Financial Support: This study was partly supported by a grant (01GI0925) from the Federal Ministry of Education and Research (BMBF) to the German Center for Diabetes Research (DZD e.V.).

Clinicaltrials.gov: NCT03637075.

Conflict of Interest: As of January 2020, B.A.J. is an employee of Eli Lilly and Company. None of the other authors report a conflict of interest in relation to this work.

Author Contributions: S.K., B.B., H.H., B.P., H.P., C.F., A.F., M.R., and M.H. designed research; B.A.J., C.G., B.B., G.R., A.F., M.R., and M.H. performed research; S.K., D.B., M.R., and M.H. analyzed data; and S.K., D.B., A.F., M.R., and M.H. wrote the paper. All authors read and approved the final manuscript.

Additional Information

Correspondence: Stephanie Kullmann, Otfried Müller str. 47, 72076 Tübingen, Germany. Email: Stephanie.kullmann@med.uni-tuebingen.de.

Data Availability: Some or all datasets generated during and/or analyzed during the current study are not publicly available but are available from the corresponding author on reasonable request.

References

1. Kullmann S, Heni M, Veit R, et al. Selective insulin resistance in homeostatic and cognitive control brain areas in overweight and obese adults. *Diabetes Care*. 2015;**38**(6):1044-1050.
2. Kullmann S, Kleinridders A, Small DM, et al. Central nervous pathways of insulin action in the control of metabolism and food intake. *Lancet Diabetes Endocrinol*. 2020;**8**(6):524-534.

3. Stoeckel LE, Arvanitakis Z, Gandy S, et al. Complex mechanisms linking neurocognitive dysfunction to insulin resistance and other metabolic dysfunction. *F1000Res*. 2016;**5**:353.
4. Biessels GJ, Reagan LP. Hippocampal insulin resistance and cognitive dysfunction. *Nat Rev Neurosci*. 2015;**16**(11):660-671.
5. Baskin DG, Porte D Jr, Guest K, Dorsa DM. Regional concentrations of insulin in the rat brain. *Endocrinology*. 1983;**112**(3):898-903.
6. Havrankova J, Roth J, Brownstein M. Insulin receptors are widely distributed in the central nervous system of the rat. *Nature*. 1978;**272**(5656):827-829.
7. Obici S, Zhang BB, Karkanias G, Rossetti L. Hypothalamic insulin signaling is required for inhibition of glucose production. *Nat Med*. 2002;**8**(12):1376-1382.
8. Brüning JC, Gautam D, Burks DJ, et al. Role of brain insulin receptor in control of body weight and reproduction. *Science*. 2000;**289**(5487):2122-2125.
9. Ferrario CR, Labouèbe G, Liu S, et al. Homeostasis meets motivation in the battle to control food intake. *J Neurosci*. 2016;**36**(45):11469-11481.
10. Liu S, Borgland SL. Insulin actions in the mesolimbic dopamine system. *Exp Neurol*. 2019;**320**:113006.
11. Ferrario CR, Reagan LP. Insulin-mediated synaptic plasticity in the CNS: anatomical, functional and temporal contexts. *Neuropharmacology*. 2018;**136**(Pt B):182-191.
12. Labouèbe G, Liu S, Dias C, et al. Insulin induces long-term depression of ventral tegmental area dopamine neurons via endocannabinoids. *Nat Neurosci*. 2013;**16**(3):300-308.
13. Mebel DM, Wong JC, Dong YJ, Borgland SL. Insulin in the ventral tegmental area reduces hedonic feeding and suppresses dopamine concentration via increased reuptake. *Eur J Neurosci*. 2012;**36**(3):2336-2346.
14. Hallschmid M. Intranasal insulin. *J Neuroendocrinol* 2021;**33**(4):e12934.
15. Kullmann S, Veit R, Peter A, et al. Dose-dependent effects of intranasal insulin on resting-state brain activity. *J Clin Endocrinol Metab*. 2018;**103**(1):253-262.
16. Lochhead JJ, Thorne RG. Intranasal delivery of biologics to the central nervous system. *Adv Drug Deliv Rev*. 2012;**64**(7):614-628.
17. Thorne RG, Pronk GJ, Padmanabhan V, Frey WH 2nd. Delivery of insulin-like growth factor-I to the rat brain and spinal cord along olfactory and trigeminal pathways following intranasal administration. *Neuroscience*. 2004;**127**(2):481-496.
18. Thorne RG, Emory CR, Ala TA, Frey WH 2nd. Quantitative analysis of the olfactory pathway for drug delivery to the brain. *Brain Res*. 1995;**692**(1-2):278-282.
19. Lochhead JJ, Kellohen KL, Ronaldson PT, Davis TP. Distribution of insulin in trigeminal nerve and brain after intranasal administration. *Sci Rep*. 2019;**9**(1):2621.
20. Born J, Lange T, Kern W, McGregor GP, Bickel U, Fehm HL. Sniffing neuropeptides: a transnasal approach to the human brain. *Nat Neurosci*. 2002;**5**(6):514-516.
21. Kullmann S, Valenta V, Wagner R, et al. Brain insulin sensitivity is linked to adiposity and body fat distribution. *Nat Commun*. 2020;**11**(1):1841.
22. Heni M, Kullmann S, Ketterer C, et al. Nasal insulin changes peripheral insulin sensitivity simultaneously with altered activity in homeostatic and reward-related human brain regions. *Diabetologia*. 2012;**55**(6):1773-1782.
23. Heni M, Wagner R, Kullmann S, Preissl H, Fritsche A. Response to Comment on Heni *et al*. Central insulin administration improves whole-body insulin sensitivity via hypothalamus and parasympathetic outputs in men. Diabetes 2014;63:4083-4088. *Diabetes*. 2015;**64**(6):e8-e9.
24. Kullmann S, Frank S, Heni M, et al. Intranasal insulin modulates intrinsic reward and prefrontal circuitry of the human brain in lean women. *Neuroendocrinology*. 2013;**97**(2):176-182.
25. Tiedemann LJ, Schmid SM, Hettel J, et al. Central insulin modulates food valuation via mesolimbic pathways. *Nat Commun*. 2017;**8**:16052.
26. Edwin Thanarajah S, Iglesias S, Kuzmanovic B, et al. Modulation of midbrain neurocircuitry by intranasal insulin. *Neuroimage*. 2019;**194**:120-127.
27. Schmid V, Kullmann S, Gfrörer W, et al. Safety of intranasal human insulin: a review. *Diabetes Obes Metab*. 2018;**20**(7):1563-1577.
28. Volkow ND, Wang GJ, Fowler JS, et al. Imaging endogenous dopamine competition with [11C]raclopride in the human brain. *Synapse*. 1994;**16**(4):255-262.
29. Narendran R, Hwang DR, Slifstein M, et al. Measurement of the proportion of D2 receptors configured in state of high affinity for agonists in vivo: a positron emission tomography study using [11C]N-propyl-norapomorphine and [11C]raclopride in baboons. *J Pharmacol Exp Ther*. 2005;**315**(1):80-90.
30. Laruelle M. Imaging synaptic neurotransmission with in vivo binding competition techniques: a critical review. *J Cereb Blood Flow Metab*. 2000;**20**(3):423-451.
31. Kullmann S, Blum D, Jaghutriz BA, et al. Supplementary data for Article: Central insulin modulates dopamine signaling in the human striatum. *Dryad, Dataset*. 2021. https://doi.org/10.5061/dryad.wstqjq2kt. Accessed June 18, 2021.
32. Pudel D, Westenhöfer J. *Fragebogen zum Eßverhalten (FEV)*. Handanweisung. Göttingen: Hogrefe, 1989.
33. Nijs IM, Franken IH, Muris P. The modified trait and state food-cravings questionnaires: development and validation of a general index of food craving. *Appetite*. 2007;**49**(1):38-46.
34. Topp CW, Østergaard SD, Søndergaard S, Bech P. The WHO-5 well-being index: a systematic review of the literature. *Psychother Psychosom*. 2015;**84**(3):167-176.
35. Heni M, Wagner R, Willmann C, et al. Insulin action in the hypothalamus increases second-phase insulin secretion in humans. *Neuroendocrinology*. 2019.
36. Malmberg A, Nordvall G, Johansson AM, Mohell N, Hacksell U. Molecular basis for the binding of 2-aminotetralins to human dopamine D2A and D3 receptors. *Mol Pharmacol*. 1994;**46**(2):299-312.
37. Langer O, Någren K, Dolle F, et al. Precursor synthesis and radiolabelling of the dopamine D2 receptor ligand [11C] raclopride from [11C]methyl triflate. *J Labelled Comp Radiopharm* 1999;**42**(12):1183-1193.
38. Innis RB, Cunningham VJ, Delforge J, et al. Consensus nomenclature for in vivo imaging of reversibly binding radioligands. *J Cereb Blood Flow Metab*. 2007;**27**(9):1533-1539.
39. Ichise M, Liow JS, Lu JQ, et al. Linearized reference tissue parametric imaging methods: application to [11C]DASB positron emission tomography studies of the serotonin

transporter in human brain. *J Cereb Blood Flow Metab*. 2003;**23**(9):1096-1112.
40. Chao-Gan Y, Yu-Feng Z. DPARSF: a MATLAB toolbox for "pipeline" data analysis of resting-state fMRI. *Front Syst Neurosci*. 2010;**4**:13.
41. Song XW, Dong ZY, Long XY, et al. REST: a toolkit for resting-state functional magnetic resonance imaging data processing. *Plos One*. 2011;**6**(9):e25031.
42. Zou QH, Zhu CZ, Yang Y, et al. An improved approach to detection of amplitude of low-frequency fluctuation (ALFF) for resting-state fMRI: fractional ALFF. *J Neurosci Methods*. 2008;**172**(1):137-141.
43. Wang Z, Aguirre GK, Rao H, et al. Empirical optimization of ASL data analysis using an ASL data processing toolbox: ASLtbx. *Magn Reson Imaging*. 2008;**26**(2):261-269.
44. Klein MO, Battagello DS, Cardoso AR, Hauser DN, Bittencourt JC, Correa RG. Dopamine: functions, signaling, and association with neurological diseases. *Cell Mol Neurobiol*. 2019;**39**(1):31-59.
45. Gautam DC. *Analysis of Insulin Receptor Function in the Central Nervous System by Conditional Inactivation of Its Gene in Mice*. 2002. University of Köln. https://kups.ub.uni-koeln.de/371/1/11v4398.pdf.
46. Lee SH, Zabolotny JM, Huang H, Lee H, Kim YB. Insulin in the nervous system and the mind: functions in metabolism, memory, and mood. *Mol Metab*. 2016;**5**(8):589-601.
47. Schilling TM, Ferreira de Sá DS, Westerhausen R, et al. Intranasal insulin increases regional cerebral blood flow in the insular cortex in men independently of cortisol manipulation. *Hum Brain Mapp*. 2013;**35**(5):1944-1956.
48. Heni M, Kullmann S, Ahlqvist E, et al. Interaction between the obesity-risk gene FTO and the dopamine D2 receptor gene ANKK1/TaqIA on insulin sensitivity. *Diabetologia*. 2016;**59**(12):2622-2631.
49. Kullmann S, Heni M, Veit R, et al. Intranasal insulin enhances brain functional connectivity mediating the relationship between adiposity and subjective feeling of hunger. *Sci Rep*. 2017;**7**(1):1627.
50. Naef L, Seabrook L, Hsiao J, Li C, Borgland SL. Insulin in the ventral tegmental area reduces cocaine-evoked dopamine in the nucleus accumbens in vivo. *Eur J Neurosci*. 2019;**50**(3):2146-2155.
51. McCaleb ML, Myers RD. Striatal dopamine release is altered by glucose and insulin during push-pull perfusion of the rat's caudate nucleus. *Brain Res Bull*. 1979;**4**(5):651-656.
52. Small DM, Jones-Gotman M, Dagher A. Feeding-induced dopamine release in dorsal striatum correlates with meal pleasantness ratings in healthy human volunteers. *Neuroimage*. 2003;**19**(4):1709-1715.
53. Wang GJ, Tomasi D, Convit A, et al. BMI modulates calorie-dependent dopamine changes in accumbens from glucose intake. *Plos One*. 2014;**9**(7):e101585.
54. Volkow ND, Wang GJ, Maynard L, et al. Brain dopamine is associated with eating behaviors in humans. *Int J Eat Disord*. 2003;**33**(2):136-142.
55. Lippert RN, Cremer AL, Edwin Thanarajah S, et al. Time-dependent assessment of stimulus-evoked regional dopamine release. *Nat Commun*. 2019;**10**(1):336.
56. Thanarajah SE, Backes H, DiFeliceantonio AG, et al. Food intake recruits orosensory and post-ingestive dopaminergic circuits to affect eating desire in humans. *Cell Metab*. 2019;**29**(3):695-706.e4.
57. Eisenstein SA, Black KJ, Samara A, et al. Striatal dopamine responses to feeding are altered in people with obesity. *Obesity (Silver Spring)*. 2020;**28**(4):765-771.
58. Kullmann S, Heni M, Hallschmid M, Fritsche A, Preissl H, Häring HU. Brain insulin resistance at the crossroads of metabolic and cognitive disorders in humans. *Physiol Rev*. 2016;**96**(4):1169-1209.
59. Kleinridders A, Pothos EN. Impact of brain insulin signaling on dopamine function, food intake, reward, and emotional behaviorI6I. *Curr Nutr Rep*. 2019;**8**(2):83-91.
60. Mizrahi R, Mamo D, Rusjan P, Graff A, Houle S, Kapur S. The relationship between subjective well-being and dopamine D2 receptors in patients treated with a dopamine partial agonist and full antagonist antipsychotics. *Int J Neuropsychopharmacol*. 2009;**12**(5):715-721.
61. Volkow ND, Wang GJ, Begleiter H, et al. High levels of dopamine D2 receptors in unaffected members of alcoholic families: possible protective factors. *Arch Gen Psychiatry*. 2006;**63**(9):999-1008.
62. Könner AC, Hess S, Tovar S, et al. Role for insulin signaling in catecholaminergic neurons in control of energy homeostasis. *Cell Metab*. 2011;**13**(6):720-728.
63. Heni M, Kullmann S, Veit R, et al. Variation in the obesity risk gene FTO determines the postprandial cerebral processing of food stimuli in the prefrontal cortex. *Mol Metab*. 2014;**3**(2):109-113.
64. Heni M, Wagner R, Kullmann S, et al. Hypothalamic and striatal insulin action suppresses endogenous glucose production and may stimulate glucose uptake during hyperinsulinemia in lean but not in overweight men. *Diabetes*. 2017;**66**(7):1797-1806.
65. Heni M, Wagner R, Kullmann S, et al. Central insulin administration improves whole-body insulin sensitivity via hypothalamus and parasympathetic outputs in men. *Diabetes*. 2014;**63**(12):4083-4088.
66. Dunn JP, Kessler RM, Feurer ID, et al. Relationship of dopamine type 2 receptor binding potential with fasting neuroendocrine hormones and insulin sensitivity in human obesity. *Diabetes Care*. 2012;**35**(5):1105-1111.
67. Xiao C, Dash S, Stahel P, Lewis GF. Effects of intranasal insulin on endogenous glucose production in insulin-resistant men. *Diabetes Obes Metab*. 2018;**20**(7):1751-1754.
68. Dash S, Xiao C, Morgantini C, Koulajian K, Lewis GF. Intranasal insulin suppresses endogenous glucose production in humans compared with placebo in the presence of similar venous insulin concentrations. *Diabetes*. 2015;**64**(3):766-774.
69. Dash S, Xiao C, Morgantini C, Koulajian K, Lewis GF. Is insulin action in the brain relevant in regulating blood glucose in humans? *J Clin Endocrinol Metab*. 2015;**100**(7):2525-2531.
70. Benedict C, Brede S, Schiöth HB, et al. Intranasal insulin enhances postprandial thermogenesis and lowers postprandial serum insulin levels in healthy men. *Diabetes*. 2011;**60**(1):114-118.
71. Iwen KA, Scherer T, Heni M, et al. Intranasal insulin suppresses systemic but not subcutaneous lipolysis in healthy humans. *J Clin Endocrinol Metab*. 2014;**99**(2):E246-E251.

72. Dunn JP, Abumrad NN, Patterson BW, Kessler RM, Tamboli RA. Brief communication: β-cell function influences dopamine receptor availability. *Plos One*. 2019;**14**(3):e0212738.
73. Plomgaard P, Hansen JS, Ingerslev B, et al. Nasal insulin administration does not affect hepatic glucose production at systemic fasting insulin levels. *Diabetes Obes Metab*. 2018;**21**(4):993-1000.
74. Ter Horst KW, Lammers NM, Trinko R, et al. Striatal dopamine regulates systemic glucose metabolism in humans and mice. *Sci Transl Med*. 2018;**10**(442):eaar3752.